

## Graphene as a transparent electrode for amorphous silicon-based solar cells

F. Vaianella, G. Rosolen, and B. Maes

Citation: *Journal of Applied Physics* **117**, 243102 (2015); doi: 10.1063/1.4923232

View online: <http://dx.doi.org/10.1063/1.4923232>

View Table of Contents: <http://scitation.aip.org/content/aip/journal/jap/117/24?ver=pdfcov>

Published by the [AIP Publishing](#)

---

### Articles you may be interested in

[Quadruple-junction thin-film silicon-based solar cells with high open-circuit voltage](#)

*Appl. Phys. Lett.* **105**, 063902 (2014); 10.1063/1.4892890

[Hot spot engineering for light absorption enhancement of solar cells with a super-structured transparent conducting electrode](#)

*Appl. Phys. Lett.* **103**, 113905 (2013); 10.1063/1.4821156

[Graphene as transparent electrode for direct observation of hole photoemission from silicon to oxide](#)

*Appl. Phys. Lett.* **102**, 123106 (2013); 10.1063/1.4796169

[Window layer with p doped silicon oxide for high  \$V\_{oc}\$  thin-film silicon n-i-p solar cells](#)

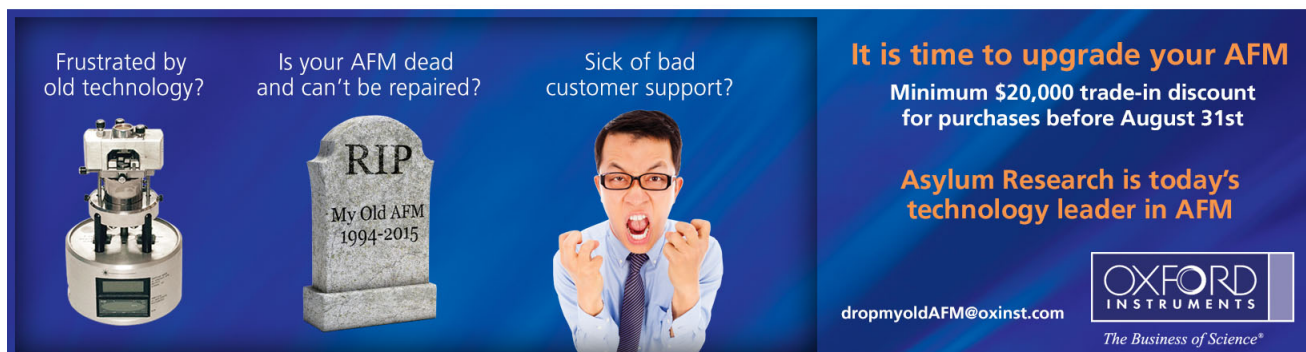
*J. Appl. Phys.* **110**, 124511 (2011); 10.1063/1.3669389

[Micromorph thin-film silicon solar cells with transparent high-mobility hydrogenated indium oxide front electrodes](#)

*J. Appl. Phys.* **109**, 114501 (2011); 10.1063/1.3592885

---

Frustrated by old technology?      Is your AFM dead and can't be repaired?      Sick of bad customer support?



**It is time to upgrade your AFM**  
Minimum \$20,000 trade-in discount for purchases before August 31st

**Asylum Research is today's technology leader in AFM**

[dropmyoldAFM@oxinst.com](mailto:dropmyoldAFM@oxinst.com)

**OXFORD INSTRUMENTS**  
The Business of Science®

# Graphene as a transparent electrode for amorphous silicon-based solar cells

F. Vaianella,<sup>a)</sup> G. Rosolen, and B. Maes

*Micro- and Nanophotonic Materials Group, Faculty of Science, University of Mons, 20 place du Parc, B-7000 Mons, Belgium*

(Received 22 January 2015; accepted 16 June 2015; published online 24 June 2015)

The properties of graphene in terms of transparency and conductivity make it an ideal candidate to replace indium tin oxide (ITO) in a transparent conducting electrode. However, graphene is not always as good as ITO for some applications, due to a non-negligible absorption. For amorphous silicon photovoltaics, we have identified a useful case with a graphene-silica front electrode that improves upon ITO. For both electrode technologies, we simulate the weighted absorption in the active layer of planar amorphous silicon-based solar cells with a silver back-reflector. The graphene device shows a significantly increased absorbance compared to ITO-based cells for a large range of silicon thicknesses (34.4% versus 30.9% for a 300 nm thick silicon layer), and this result persists over a wide range of incidence angles. © 2015 AIP Publishing LLC.

[<http://dx.doi.org/10.1063/1.4923232>]

## I. INTRODUCTION

Even if crystalline silicon (cSi) has a larger region of absorbing wavelengths, amorphous silicon (aSi) has the interesting advantages of being cheaper to produce and having a more efficient absorption (Fig. 1), which reduces the material thickness and the production price.<sup>1,2</sup> However, the diffusion length of free carriers is much smaller in the amorphous phase, thus these cells require complete surface-covering electrodes.

Graphene is a two-dimensional honeycomb lattice of carbon atoms whose electrical and optical properties have been studied intensively over the last decade.<sup>4-7</sup> Its valence and conduction bands touch each other, making it a gapless semiconductor<sup>8</sup> with high conductivity, mechanical flexibility, and optical transparency.<sup>9</sup> The properties of graphene lead to large expectations for devices such as liquid crystal displays, photovoltaic cells and light-emitting diodes (LEDs).<sup>10,11</sup>

Several techniques for growing graphene layers such as exfoliation from graphite,<sup>12-14</sup> chemical vapor deposition,<sup>15-17</sup> and thermal decomposition on SiC substrates<sup>18-20</sup> are well mastered and allow to obtain relatively low cost and large scale production of electrodes, making it a potential substitute for the expensive indium tin oxide (ITO) based electrodes, the current leader in the industry.<sup>21</sup>

Experimental and numerical studies of graphene electrodes for organic solar cells show that the power conversion efficiency can compete with ITO-based cells.<sup>16,17,22</sup> In addition, it was demonstrated that graphene keeps its electrical and optical properties even when coated on (amorphous or crystalline) silicon.<sup>23</sup> Furthermore, graphene is electrically adapted to act as an electrode for amorphous-based solar cells and shows similar electrical characteristic than ITO, even without doping.<sup>24</sup> However, in order to decrease the absorption of the graphene layers, one should limit the number of layers needed by doping the graphene.<sup>25</sup> In 2012, Zhao *et al.* have demonstrated via finite-difference time-domain (FDTD) simulations

that the optical absorption of a simple structure of amorphous silicon with only graphene on the top is worse than with a 20 nm thick ITO electrode on the top<sup>26</sup> because graphene leads to a higher reflection of the incident light than ITO. Nevertheless, the performances of graphene can overcome those of ITO by using an anti-reflective coating made of a SiO<sub>2</sub>/SiC structure.

In this paper, we investigate the optical potential of a graphene surface-covering electrode for planar amorphous silicon-based solar cells, as an alternative for the usual ITO electrode (typical structures in Fig. 2). We determine that graphene, in a suitable multilayer structure with anti-reflecting properties, can enhance or at least compete with the absorption of an ITO electrode, for an amorphous silicon active layer with various thicknesses. These enhancements persist for large angles of incidence, even up to 70°. For these studies, we perform extensive numerical simulations (commercial software COMSOL Multiphysics.<sup>27</sup>).

The paper is structured as follows. Section II reviews the optical properties of graphene. In Sec. III, we determine the absorbance of the active material when an ITO electrode is used. As ITO also functions as an anti-reflective coating, we introduce an anti-reflective silicon oxide (SiO<sub>2</sub>) layer in Sec. IV, which is subsequently coupled with graphene in Sec. V. The angular dependence is discussed in Sec. VI. Finally, we discuss the influence of the silicon thickness in Sec. VII.

## II. OPTICAL PROPERTIES OF GRAPHENE

The permittivity  $\epsilon$  of graphene is related to its optical surface conductivity  $\sigma$ <sup>28</sup>

$$\epsilon(\omega, E_F) = 1 + i \frac{\sigma(\omega, E_F)}{\epsilon_0 \omega d}, \quad (1)$$

with  $\omega$  the angular frequency,  $E_F$  the doping level, and  $d$  the thickness of graphene used for simulations. A thickness  $d = 0.5$  nm is well converged with respect to the limit  $d \rightarrow 0$ , so

<sup>a)</sup>Electronic mail: Fabio.Vaianella@umons.ac.be

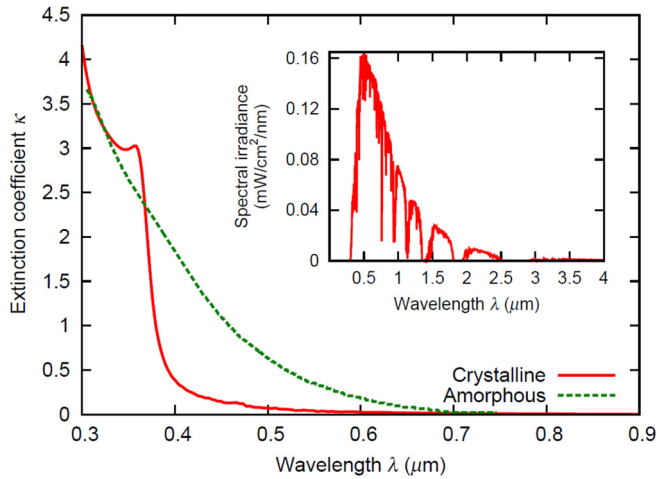


FIG. 1. Extinction coefficient of both crystalline (red solid line) and amorphous (green dashed line) silicon.<sup>2,3</sup> The absorption is greater for the amorphous phase from 370 to 750 nm. Inset shows the air mass 1.5 global (AM1.5G) solar spectrum.

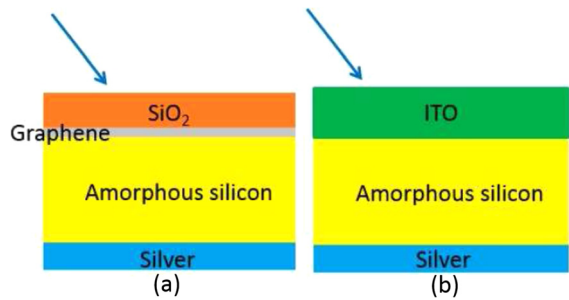
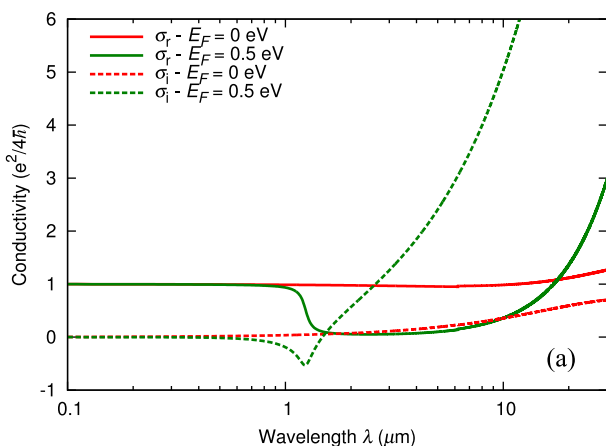


FIG. 2. Structures under study. (a) Graphene-based electrode with a SiO<sub>2</sub> anti-reflective coating on an amorphous silicon layer and a silver back-reflector. (b) ITO-based electrode on the same cell. The (blue) arrows indicate the illumination direction.

we use this value for the simulations. The optical surface conductivity can be calculated using the Kubo-Greenwood formula<sup>29–32</sup>

$$\sigma = \sigma_{intra} + \sigma_{inter}, \quad (2)$$



with

$$\sigma_{intra} = \frac{2ie^2k_B T}{\hbar^2 \pi (\omega + i\tau^{-1})} \ln \left[ 2 \cosh \left( \frac{E_F}{2k_B T} \right) \right], \quad (3)$$

$$\sigma_{inter} = \frac{e^2}{4\hbar} \left[ \frac{1}{2} + \frac{1}{\pi} \arctan \left( \frac{\hbar\omega - 2E_F}{2k_B T} \right) \right] - \frac{e^2}{4\hbar} \left[ \frac{i}{2\pi} \ln \frac{(\hbar\omega + 2E_F)^2}{(\hbar\omega - 2E_F)^2 + (2k_B T)^2} \right], \quad (4)$$

with  $\sigma_{intra}$  the conductivity related to the intraband electron-photon scattering processes,  $\sigma_{inter}$  related to the interband electron transitions,  $\tau$  the electron scattering lifetime,  $T$  the temperature (we use room temperature here), and  $k_B$  the Boltzmann constant. We use the parameters given by Eqs. (1) and (2) to simulate graphene (Fig. 3(a)).

Although a single layer of graphene is only one atom thick, its absorbance in the visible and at higher frequencies is constant, determined by the fine structure constant  $\alpha$  so that  $A \approx \pi\alpha \approx 2.3\%$ .<sup>33,34</sup> Fig. 3(b) shows that the absorbance of a single layer of graphene with air above and below is constant over the region where amorphous silicon can absorb the most light ( $\approx 300\text{--}750$  nm), and is independent of the doping level for this range (except for a doping level higher than  $E_F = 1$  eV, but this doping level is hard to achieve in practice). So, Figs. 3(a) and 3(b) show that for achievable doping levels ( $E_F < 1$  eV), the optical properties of graphene do not depend on the doping in the studied wavelength range. Doping level effects are notable only in the near and far infrared range. We can thus omit the doping level for the optical study.

### III. ITO ON AMORPHOUS SILICON

In order to compare devices with ITO and graphene, we simulate the absorbance for both electrodes of a 300 nm thick layer of amorphous silicon with a silver back-reflector, illuminated with a monochromatic plane wave at normal incidence (angle dependence is considered in Sec. VI) with wavelengths from 300 to 750 nm (spectral range for

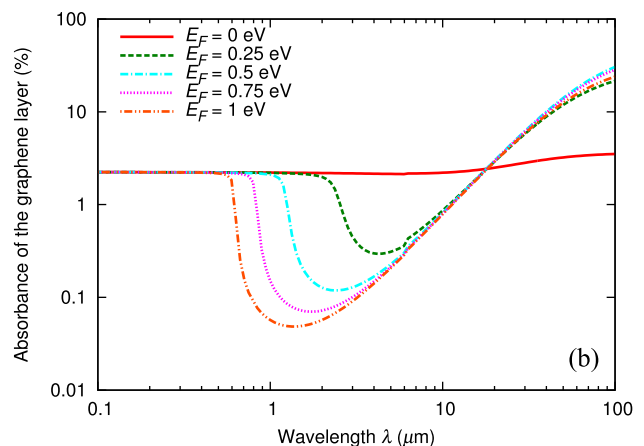


FIG. 3. (a) Real part (solid line) and imaginary part (dashed line) of the conductivity of a single layer of graphene with (green) and without (red) doping. In the visible range, doping has no effect. (b) Absorbance of a single layer of graphene at normal incidence for different doping levels  $E_F$  from 0 to 1 eV. In the visible range, the absorbance is approximately constant ( $=\pi\alpha$ ) and is independent of the doping level.

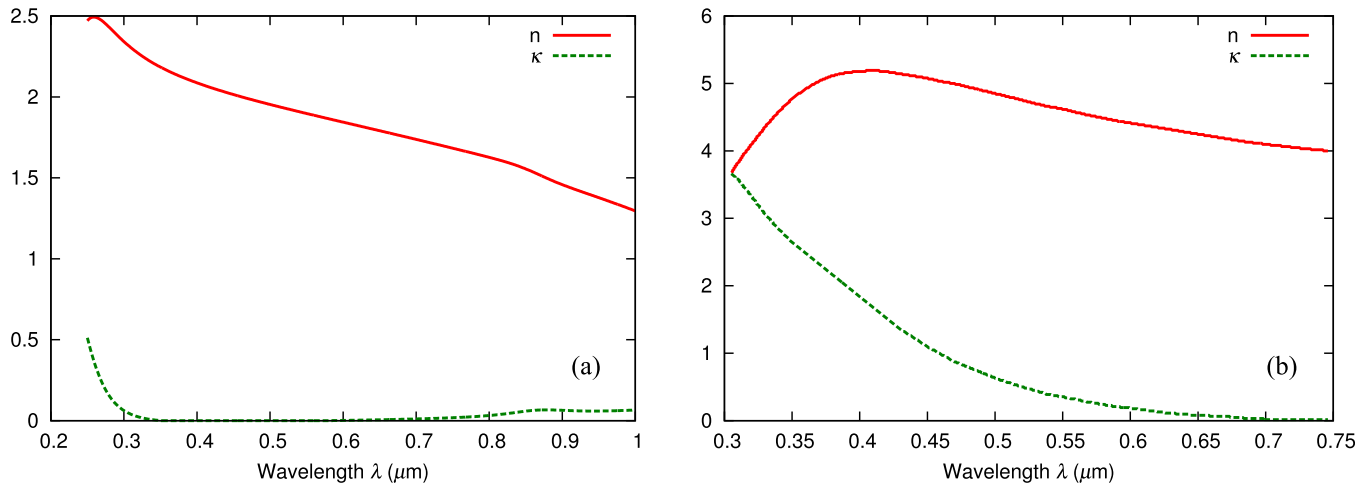


FIG. 4. Optical parameters (refractive index  $n$  and extinction coefficient  $\kappa$ ) of (a) ITO and (b) amorphous silicon.

non-negligible absorption). Other silicon thicknesses are discussed in Sec. VII. The graphene-based and ITO-based structures are shown in Figs. 2(a) and 2(b), respectively. In this section, we show results for ITO; Section V will discuss the graphene electrode. Silver optical parameters are from Ref. 35. The optical parameters of ITO<sup>36</sup> and amorphous silicon are shown in Figs. 4(a) and 4(b), respectively. We see that the extinction coefficient  $\kappa$  of ITO is practically zero in the range from 300 to 800 nm.

We calculate the integral absorbance  $A_{int}$  in the active material (thus, only silicon absorbance, not absorbance in the electrode), which is the absorbance weighted by the air mass 1.5 global (AM1.5G) solar spectrum (see inset of Fig. 1)

$$A_{int} = \frac{\int_{300\text{ nm}}^{750\text{ nm}} S(\lambda)A(\lambda)d\lambda}{\int_{300\text{ nm}}^{4000\text{ nm}} S(\lambda)d\lambda}, \quad (5)$$

where  $\lambda$  is the free-space wavelength of the incoming light,  $A(\lambda)$  is the wavelength-dependent absorbance of the silicon layer, and  $S(\lambda)$  is the AM1.5G solar spectrum.

Note that with this definition, even if all incoming light is absorbed ( $A(\lambda) = 1$ ) in the range 300–750 nm, the integral absorbance would be 53.6%.

We can now determine the ideal thickness of the ITO layer in order to compare with graphene-based devices in optimal conditions. Fig. 5 shows the integral absorbance for the ITO-based structure in function of the ITO layer thickness. A peak in absorbance is observed around a thickness of 60 nm. This is linked to the fact that the maximum of the solar spectrum is around a wavelength of 500 nm and the classical thickness condition for the most efficient anti-reflective coating (ARC) is:

$$d = \frac{\lambda}{4n}, \quad (6)$$

with  $d$  the thickness of the ARC and  $n$  its refractive index, which gives effectively  $d \approx 60$  nm as ideal thickness.

Even if 60 nm is optically optimal, one should also take care of the conducting performance of the electrode. This

performance for ITO layers is generally considered satisfactory around a thickness of 100 nm (sheet resistance  $\approx 30 \Omega/\square$ ).<sup>10,22</sup>

Thus, taking into account optical, electrical, and economic arguments, we take an ITO thickness of 100 nm for the electrode (a thicker layer than 170 nm would be more efficient but too expensive). This leads finally to an integral absorbance of 30.9%. Sections IV and V will demonstrate that the integral absorbance of graphene-based devices can exceed this value.

#### IV. SiO<sub>2</sub> ON AMORPHOUS SILICON

Because of its extreme thinness, we can at first neglect the graphene layer in Fig. 2(a), in order to determine the optimal thickness of the necessary silica ARC. The silica refractive index does not vary much, so we consider a constant value of 1.5.

Fig. 6 shows the evolution of the integral absorbance of silicon as the thickness of the oxide increases. A peak is observed around a thickness of 80 nm that, again, is in good agreement with Eq. (6). The integral absorbance in this best

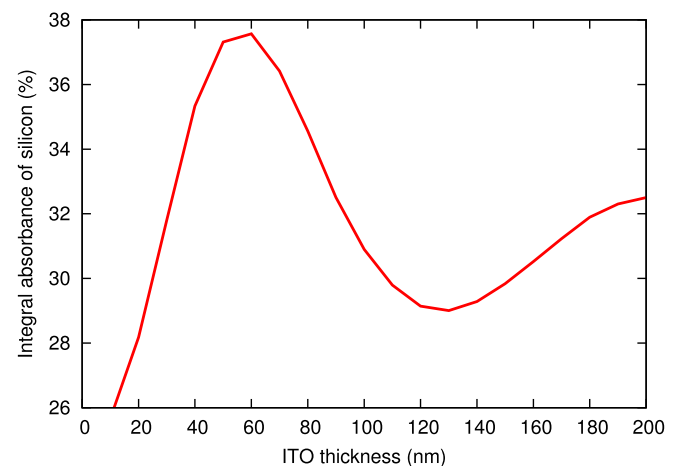


FIG. 5. Integral absorbance  $A_{int}$  of silicon weighted with AM1.5G solar spectrum for a ITO/amorphous silicon/silver structure as a function of the ITO layer thickness, under normal incidence.

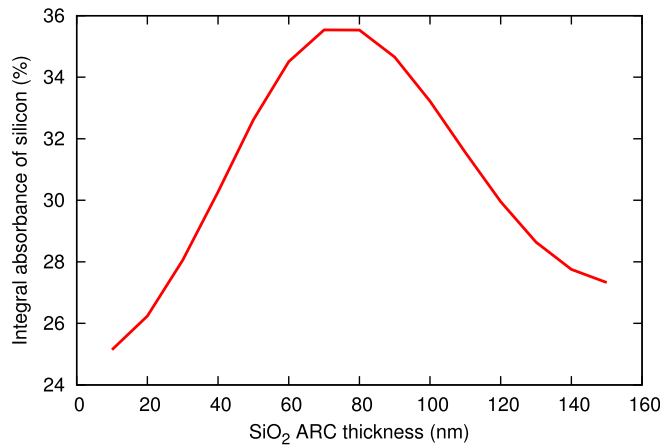


FIG. 6. Integral absorbance  $A_{int}$  for a SiO<sub>2</sub>/amorphous silicon/silver structure, as a function of the SiO<sub>2</sub> anti-reflective coating thickness, under normal incidence.

configuration is around 35.5%, which is larger than the ITO-based configuration (30.9%).

This difference is mainly due to a larger reflection of ITO between 370 and 580 nm and also between 610 and 650 nm, which are important parts of the AM1.5 G spectrum, see Fig. 7 for the reflectance spectra.

## V. SiO<sub>2</sub>/GRAPHENE ON AMORPHOUS SILICON

We now examine the structure by adding the electrode of graphene (Fig. 2(a)). Fig. 8 shows the silicon absorbance for various numbers of graphene layers. Even with ten layers, the graphene structure gives a larger absorbance in the silicon than the ITO-based one. Each graphene layer absorbs only about 0.3% of the light, which is much less than the 2.3% for graphene surrounded with air (see Sec. II). This decrease in absorbance of a single graphene layer is due to a decrease of the electric field at the graphene boundary (directly connected with absorption<sup>28</sup>) with an increase of the refractive index of the substrate on which the layer is deposited because of interference with the reflected field. The real part of the refractive index of silicon being much higher than that of air over all the wavelengths of interest, the

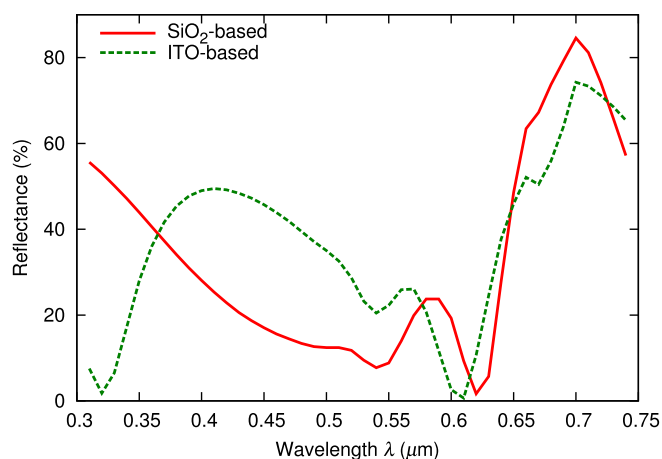


FIG. 7. Reflectance spectra of both structures under normal incidence with ITO and SiO<sub>2</sub>. Red solid line is for a 80 nm thick SiO<sub>2</sub> layer. Green dashed line is for a 100 nm thick ITO layer.

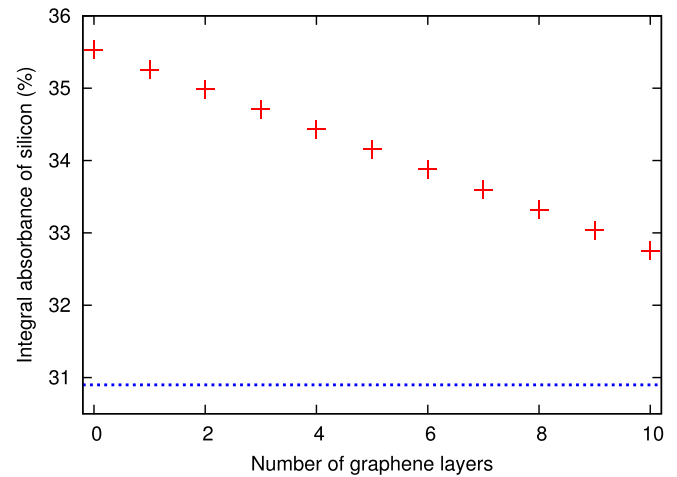


FIG. 8. Red points indicate the integral absorbance  $A_{int}$  for SiO<sub>2</sub>/graphene/amorphous silicon/silver as a function of the number of graphene layers composing the electrode. For comparison, the blue dotted line indicates the absorbance of the ITO structure.

absorbance of the graphene layer decreased significantly. The latter result shows that multilayer optimization is important for graphene devices.

The sheet resistance of a single graphene layer with doping level  $E_F = 0.3$  eV being  $\approx 120 \Omega/\square$ , at least four layers are needed in order to have a satisfactory conduction, with a sheet resistance of  $\approx 30 \Omega/\square$ .<sup>10,22,37</sup> With four layers, the absorbance is around 34.4%, giving an optical enhancement of 3.5% compared to photovoltaic cells with an ITO electrode, which is an interesting result. Note that a (quite expensive) ITO thickness of 200 nm (maximum point in Fig. 5) would still be worse than a four-layer graphene electrode: 32.5% versus 34.4%.

## VI. ANGLE DEPENDENCE

The superiority of graphene at normal incidence being established, the structure should be efficient for a large range of incidence angles for photovoltaics (from 0° to 60° is, in general, suitable). We study the same structures as previously, but we vary the angle of incidence from 0 to 90°.

The incidence angle does not have much effect on the graphene device until 60° (Fig. 9(b)), while an increase in absorbance is observed for the TM polarisation of the ITO structure (Fig. 9(a)). The latter increase is connected with an increased transmission in the structure due to the pseudo-Brewster angle (between ITO and silicon), which is the angle where the reflection of the TM polarisation vanishes.

We consider the mean integral absorbance (Fig. 10) given by

$$A_{mean} = \frac{A_{TM} + A_{TE}}{2}, \quad (7)$$

with  $A_{TM}$  ( $A_{TE}$ ) the integral absorbance for TM (TE) polarisation. With ITO, there is a slight increase in absorbance in function of the angle. However, graphene is more efficient for angles up to 70°. For larger angles than 70°, the performance is similar. The absorbance of the graphene cell is almost

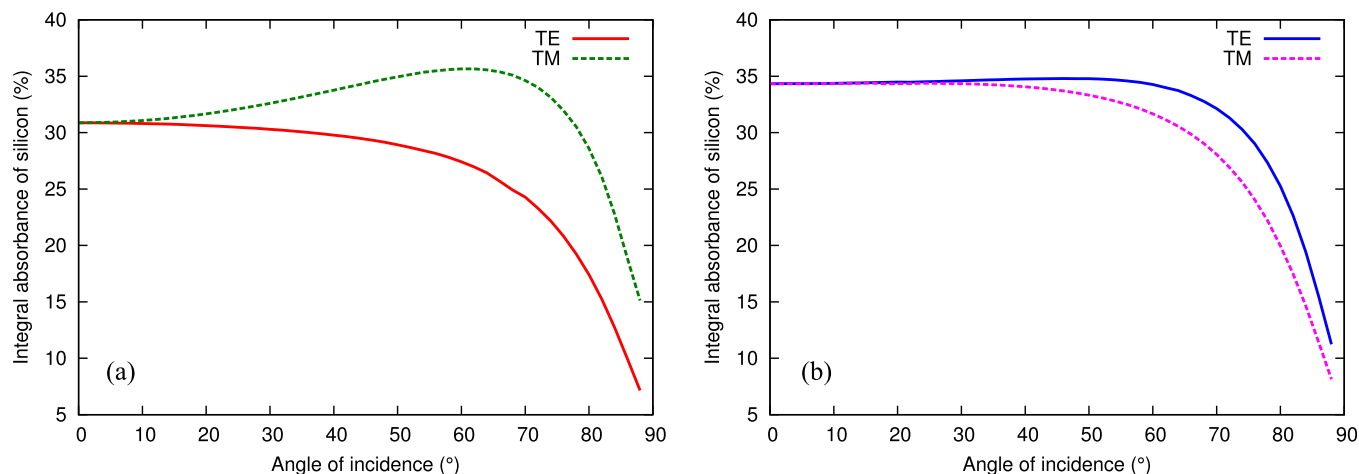


FIG. 9. Influence of the incidence angle on the integral absorbance  $A_{int}$  for TM (dashed line) and TE (solid line) polarisation. (a) ITO electrode. (b) Graphene electrode.

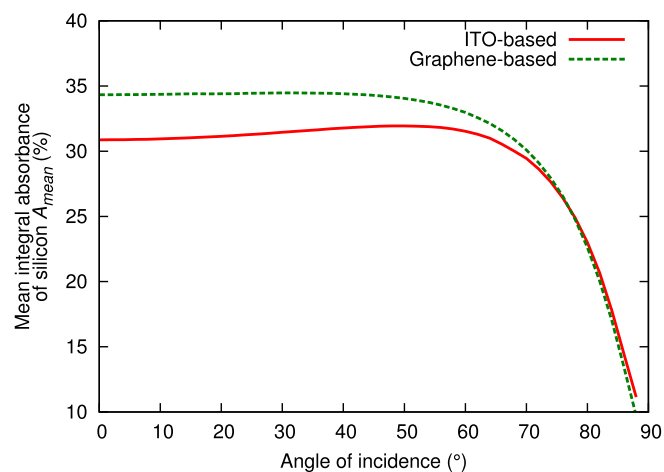


FIG. 10. Influence of the incidence angle on the mean absorbance of ITO and graphene devices. Red solid line is for ITO, green dashed line for graphene.

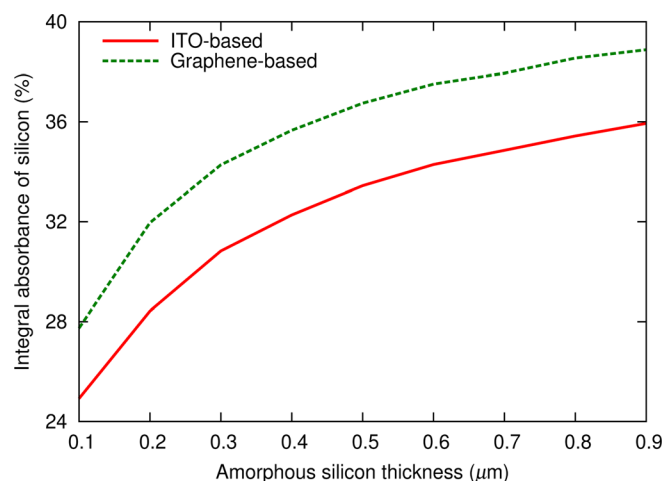


FIG. 11. Influence of the silicon thickness on the absorbance of the active layer. Red solid line is for the ITO-based structure; green dashed line is for the graphene-based structure.

constant from 0 to  $50^\circ$ , allowing for flexibility in photovoltaic panel orientation.

## VII. INFLUENCE OF THE SILICON THICKNESS

We have determined that graphene could enhance the absorbance in the amorphous silicon layer when its thickness is 300 nm. However, this thickness is not necessarily the thickness required for some applications. We study the influence of the silicon thickness by varying it from 100 to 900 nm. As indicated by equation 6, the ideal ARC thickness does not depend much on the silicon thickness. We thus use a 80 nm layer of  $\text{SiO}_2$  and a 100 nm layer of ITO as previously.

Fig. 11 shows the integral absorbance of silicon versus its thickness. We see that the integral absorbance for the graphene-based structure is always higher than the ITO-based structure (in this range of thicknesses), with a gain going from 2.8% to 3.5%. The absorbance increases with the silicon thickness, as one intuitively expects.

## VIII. CONCLUSIONS

We numerically demonstrate that the electrical and optical properties of graphene are suitable as transparent conducting electrode for thin-film amorphous silicon photovoltaics. The weighted absorbance in the active material with a four-layer graphene electrode (which provides a good electrical conduction) is larger than with an ITO electrode for a silicon thickness going from 100 to 900 nm. An increase in absorbance up to 3.5% is achievable. Moreover, the graphene electrode keeps its efficiency over a large range of incidence angles, up to  $70^\circ$ .

These results depend on the ability to fabricate structures with graphene in between amorphous silicon and an anti-reflective coating, which is crucial for optical performance. A device with graphene in between  $\text{SiO}_2$  and quartz was fabricated<sup>38</sup> for example, so the proposed structure should become realizable. In that case, it would provide an inexpensive and efficient alternative for the transparent conducting electrode.

## ACKNOWLEDGMENTS

This work was supported by the Belgian Science Policy Office under the project “Photonics@be” (P7-35) and by the Fonds pour la Formation à la Recherche dans l’Industrie et dans l’Agriculture (FRIA) in Belgium.

- <sup>1</sup>L. Yang, Y. Xuan, and J. Tan, *Opt. Express* **19**, A1165 (2011).
- <sup>2</sup>Y. Park, E. Drouard, O. El Daif, X. Letartre, P. Viktorovitch, A. Fave, A. Kaminski, M. Lemiti, and C. Seassal, *Opt. Express* **17**, 14312 (2009).
- <sup>3</sup>G. Vuye, S. Fisson, V. N. Van, Y. Wang, J. Rivory, and F. Abeles, *Thin Solid Films* **233**, 166 (1993).
- <sup>4</sup>X. Li, H. Zhu, K. Wang, A. Cao, J. Wei, C. Li, Y. Jia, Z. Li, X. Li, and D. Wu, *Adv. Mater.* **22**, 2743 (2010).
- <sup>5</sup>Q. Bao and K. P. Loh, *ACS Nano* **6**, 3677 (2012).
- <sup>6</sup>R. Won, *Nat. Photonics* **4**, 411 (2010).
- <sup>7</sup>F. Bonaccorso, Z. Sun, T. Hasan, and A. C. Ferrari, *Nat. Photonics* **4**, 611 (2010).
- <sup>8</sup>S. Tongay, M. Lemaitre, X. Miao, B. Gila, B. Appleton, and A. Hebard, *Phys. Rev. X* **2**, 011002 (2012).
- <sup>9</sup>P. Avouris and M. Freitag, *IEEE J. Sel. Top. Quantum Electron.* **20**, 72 (2014).
- <sup>10</sup>G. Jo, M. Choe, S. Lee, W. Park, Y. H. Kahng, and T. Lee, *Nanotechnology* **23**, 112001 (2012).
- <sup>11</sup>J. Wu, M. Agrawal, H. A. Becerril, Z. Bao, Z. Liu, Y. Chen, and P. Peumans, *ACS Nano* **4**, 43 (2010).
- <sup>12</sup>X. Wang, L. Zhi, and K. Mullen, *Nano Lett.* **8**, 323 (2008).
- <sup>13</sup>K. Parvez, Z.-S. Wu, R. Li, X. Liu, R. Graf, X. Feng, and K. Mullen, *J. Am. Chem. Soc.* **136**, 6083 (2014).
- <sup>14</sup>M. Lotya, Y. Hernandez, P. J. King, R. J. Smith, V. Nicolosi, L. S. Karlsson, F. M. Blighe, S. De, Z. Wang, I. T. McGovern, G. S. Duesberg, and J. N. Coleman, *J. Am. Chem. Soc.* **131**, 3611 (2009).
- <sup>15</sup>E. Shi, H. Li, L. Yang, L. Zhang, Z. Li, P. Li, Y. Shang, S. Wu, X. Li, J. Wei, K. Wang, H. Zhu, D. Wu, Y. Fang, and A. Cao, *Nano Lett.* **13**, 1776 (2013).
- <sup>16</sup>L. Gomez De Arco, Y. Zhang, C. W. Schlenker, K. Ryu, M. E. Thompson, and C. Zhou, *ACS Nano* **4**, 2865 (2010).
- <sup>17</sup>H. Park, J. A. Rowehl, K. K. Kim, V. Bulovic, and J. Kong, *Nanotechnology* **21**, 505204 (2010).
- <sup>18</sup>K. Emtsev, F. Speck, Th. Seyller, L. Ley, and J. Riley, *Phys. Rev. B* **77**, 155303 (2008).
- <sup>19</sup>C. Xia, L. I. Johansson, Y. Niu, A. A. Zakharov, E. Janzen, and C. Virojanadara, *Carbon* **79**, 631 (2014).
- <sup>20</sup>H. Hibino, S. Tanabe, S. Mizuno, and H. Kageshima, *J. Phys. D* **45**, 154008 (2012).
- <sup>21</sup>A. Kumar and C. Zhou, *ACS Nano* **4**, 11 (2010).
- <sup>22</sup>W. S. Koh, C. H. Gan, W. K. Phua, Y. A. Akimov, and P. Bai, *IEEE J. Sel. Top. Quantum Electron.* **20**, 36 (2014).
- <sup>23</sup>M. A. Gluba, D. Amkreutz, G. V. Troppenz, J. Rappich, and N. H. Nickel, *Appl. Phys. Lett.* **103**, 073102 (2013).
- <sup>24</sup>M. Schriver, W. Regan, M. Loster, and A. Zettl, *Solid State Commun.* **150**, 561 (2010).
- <sup>25</sup>Y. Khatami, W. Liu, J. Kang, and K. Banerjee, *SPIE Proc.* **8824**, 88240T-1–88240T-6 (2013).
- <sup>26</sup>Y. Zhao, F. Chen, Q. Shen, and L. Zhang, *Appl. Opt.* **51**, 6245 (2012).
- <sup>27</sup>COMSOL Multiphysics 4.4c., <http://www.comsol.com/>.
- <sup>28</sup>L. D. Landau and E. M. Lifshitz, *Electrodynamics of Continuous Media* (Pergamon Press, 1984).
- <sup>29</sup>A. Y. Nikitin, F. Guinea, F. Garcia-Vidal, and L. Martin-Moreno, *Phys. Rev. B* **84**, 195446 (2011).
- <sup>30</sup>L. A. Falkovsky and A. A. Varlamov, *Eur. Phys. J. B* **56**, 281 (2007).
- <sup>31</sup>C. H. Gan, H. S. Chu, and E. P. Li, *Phys. Rev. B* **85**, 125431 (2012).
- <sup>32</sup>L. A. Falkovsky, *J. Phys.: Conf. Ser.* **129**, 012004 (2008).
- <sup>33</sup>R. Kumar, A. K. Sharma, M. Bhatnagar, B. R. Mehta, and S. Rath, *Nanotechnology* **24**, 165402 (2013).
- <sup>34</sup>R. R. Nair, P. Blake, A. N. Grigorenko, K. S. Novoselov, T. J. Booth, T. Stauber, N. M. R. Peres, and A. K. Geim, *Science* **320**, 1308 (2008).
- <sup>35</sup>A. D. Rakic, A. B. Djuricic, J. M. Elazar, and M. L. Majewski, *Appl. Opt.* **37**, 5271 (1998).
- <sup>36</sup>Data from IMEC.
- <sup>37</sup>C. Xu, H. Li, and K. Banerjee, *IEEE Trans. Electron Devices* **56**, 1567 (2009).
- <sup>38</sup>G. Pirruccio, L. M. Moreno, G. Lozano, and J. G. Rivas, *ACS Nano* **7**, 4810 (2013).